Title

Neural measures associated with configural threat acquisition

Authors

Stout, Daniel M
Glenn, Daniel E
Acheson, Dean T
et al.

Publication Date

2018-04-01

DOI

10.1016/j.nlm.2018.03.012

Peer reviewed

Published in final edited form as:
Neurobiol Learn Mem. 2018 April ; 150: 99–106. doi:10.1016/j.nlm.2018.03.012.

Neural Measures Associated with Configural Threat Acquisition

Daniel M. Stout[1,2], **Daniel E. Glenn**[1,2], **Dean T. Acheson**[1,2], **Andrea D. Spadoni**[1,2], **Victoria B. Risbrough**[1,2,†], **Alan N. Simmons**[1,2,†,*]

[1]Center of Excellence for Stress and Mental Health, VA San Diego Healthcare System, San Diego, CA 92161 USA

[2]Department of Psychiatry, University of California San Diego, San Diego, CA 92093 USA

Abstract

Contextual threat learning reflects two often competing processes: configural and elemental learning. Configural threat learning is a hippocampal-dependent process of forming a conjunctive representation of a context through binding of several multi-modal elements. In contrast, elemental threat-learning is governed by the amygdala and involves forming associative relationships between individual features within the context. Contextual learning tasks in humans however, rarely probe if a learned fear response is truly due to configural learning vs. simple elemental associations. The aim of the current study was to probe both constructs separately to enable a more refined interpretation of configural vs. elemental threat learning performance and mediating circuits. Subjects (n=25) performed both a novel feature-identical contextual threat conditioning task and a discrete cue threat acquisition task while undergoing functional magnetic resonance imaging. Results demonstrated increased hippocampus activity for the threat configuration compared to the safe configuration. This pattern was not observed in the amygdala. In contrast, elemental threat learning was associated with increased amygdala, but not hippocampus activity. Whole-brain analyses revealed that both configural and elemental threat acquisition share neural circuitry related to fear expression. These results provide support for the importance of the hippocampus specifically in configural threat acquisition and fear expression.

Keywords

Fear; Context; Configural; fMRI; Hippocampus; Conditioning

1. INTRODUCTION

Learning about and predicting threat is important for adaptive functioning, both in terms of discrete cues associated with threat, and also the surrounding context within which threat occurs (Maren, Phan, & Liberzon, 2013). Context shapes perception and selection

[*]Corresponding author Dr. Alan Simmons (ansimmons@ucsd.edu), Associate Professor, Department of Psychiatry, UCSD, Research Scientist, VA San Diego Healthcare System, 3350 La Jolla Village Drive, San Diego, CA 92161, Phone: 858-642-3547; Fax: 858-534-9450.
[†]Both authors contributed equally to this work

CONFLICT OF INTEREST STATEMENT
The authors declare that they have no competing or conflicts of interests.

of appropriate cognitive, behavioral, and neurobiological responses (Chun & Phelps, 1999). Understanding the neural mechanisms of contextual threat learning may accelerate our capacity to treat psychiatric disorders that have known deficits in contextual threat learning, such as posttraumatic stress disorder (Acheson, Gresack, & Risbrough, 2012; Liberzon & Abelson, 2016).

Animal studies indicate that contextual threat may be learned through two distinct processes: elemental and configural threat learning (Rudy, Huff, & Matus-Amat, 2004). Elemental learning is an amygdala-dependent process which involves forming discrete Pavlovian associations with one or more salient cues in the environment during the aversive event (Davis & Whalen, 2001; LeDoux, 2000; Urcelay & Miller, 2014). These associations are context independent, in that the elemental cue can trigger a fear response in varied environments. Alternatively, configural learning reflects the integration of individual multimodal elements into a single overall representation of the environment or “context” in which the aversive event occurs (Rudy, 2009). The hippocampus supports configural representations via relational and spatial binding of multimodal stimuli (Eichenbaum & Cohen, 2014.; Monti et al., 2015). Configural and elemental processes compete over representation of contextual information such that under normal circumstances hippocampal-driven configural learning takes priority by creating a conjunctive representation of the whole context and then is assigned the associative strength, rather than the individual elements (Fanselow, 2000). The hippocampus modulates amygdala-driven learned fear responses via reciprocal connections to the amygdala and cortex (Nees & Pohlack, 2014; Olsen, Moses, Riggs, & Ryan, 2012). However, if there is impaired functioning of the hippocampus then contextual information can be represented, almost solely, through amygdala-driven elemental learning, which increases the likelihood of an individual element from the environment in which the aversive event was experienced to subsequently trigger a fear response (Maren, Aharonov, & Fanselow, 1997; Maren et al., 2013).

The relationship between configural and elemental contextual threat learning has important theoretical implications for the etiology and maintenance of PTSD. Investigators have argued that many PTSD-related re-experiencing and hyperarousal symptoms are associated with a break-down of the hippocampal-configural threat learning process, leading to an overreliance of elemental processing subserved by the amygdala (Acheson et al., 2012; Liberzon & Abelson, 2016). Loss of contextual threat discrimination over time is associated with fear generalization in novel contexts, a key feature of PTSD and anxiety-related disorders (Andreatta, Neueder, Glotzbach-Schoon, Mühlberger, & Pauli, 2017; Lissek, 2012). Thus, there is a great deal of interest in better understanding hippocampus-dependent configural processes of contextual threat conditioning in human populations (Stark, Reagh, Yassa, & Stark, 2017).

Many of the fMRI investigations using unpredictable shock, colored backgrounds, static rooms, or virtual reality contexts generally support the role of the hippocampus and amygdala in contextual threat conditioning (Alvarez, Biggs, Chen, Pine, & Grillon, 2008; Barrett & Armony, 2009; Pohlack, Nees, Ruttorf, Schad, & Flor, 2012). These studies utilize experimental designs that manipulate multiple distinct contextual characteristics (US

unpredictability, long stimulus duration, multimodal configuration) making it difficult to distinguish between configural or elemental learning (for review see Glenn, Risbrough, Simmons, Acheson, & Stout, 2017). Therefore, before gaining a better understanding of the neural circuitry associated with contextual threat learning, work is needed to delineate how individuals process the multiple cues in the environment. One way of addressing this methodological limitation is to develop feature-identical positive and negative conditioned stimuli that require configural learning of the overall arrangement of contextual elements to accurately predict the likelihood of an aversive event. Baeuchl and colleagues (2015) completed the first neuroimaging study of configural threat conditioning to utilize a feature-identical paradigm, with the threat context comprised of several elements, and the safe context comprised of a different configuration of the same elements. Consistent with theoretical models of configural processing, the authors found increased hippocampus activity for the threat configuration relative to safe configuration. However, a limitation of this paradigm is that differentiating threat from safety did not necessitate learning a representation of the entire context, as contextual discrimination could be accomplished based on learning only a pair of elements. Moreover, Baeuchl and colleagues (2015) did not compare configural threat learning with elemental learning, which limits the conclusions that can be made regarding the neural observations reported.

The current investigation aimed to address the limitations noted above by utilizing a novel feature-identical paradigm to examine the neural measures associated with configural threat acquisition. Here, subjects completed separate configural and elemental threat conditioning tasks (Baeuchl, Meyer, Hoppstädter, Diener, & Flor, 2015; Glenn et al., in press) while recording functional magnetic resonance imaging (fMRI) and skin conductance response (SCR). Rather than examining the background context, the configural task was designed to require configural processing of multiple cues in order to discriminate threat from safety, thus we did not measure contextual threat learning as done in other studies (Alvarez et al., 2008; Lang et al., 2009; Marschner, Kalisch, Vervliet, Vansteenwegen, & Büchel, 2008). Instead, this approach allowed identification and comparison of the neural circuitry associated with configural threat learning versus elemental threat learning. We hypothesized that configural threat learning will be associated with hippocampus and amygdala activity while elemental threat learning would rely on the amygdala but not the hippocampus.

2. MATERIALS AND METHOD

2.1 Participants

A total of 25 subjects (mean age=34.57, *SD*=10.13, range= 19–50; 10 female) from the San Diego area completed separate configural and elemental threat learning tasks while undergoing fMRI. One subject was removed due to excessive scanner artifact, leaving 24 subjects for the imaging analyses. An additional 4 subjects were removed from the SCR analyses due to technical problems. Informed consent was obtained from all subjects prior to participating. The institutional review board of the University of California San Diego approved all study procedures.

2.2 Threat Conditioning Tasks

The configural and elemental tasks (see Fig. 1) were completed separately with the order counterbalanced across subjects. During both tasks, a white fixation cross against a black background was presented for 10 to 14-s during inter-stimulus intervals (ISI). The order of reinforced and non-reinforced trials was randomized and counterbalanced across subjects in each task, with no stimulus type appearing more than twice consecutively. The aversive unconditional stimulus (US) was a 250-psi air-puff delivered via a plastic tube positioned 2.5 cm from the center of the throat.

Configural.—Stimuli consisted of computer-generated pictures of a room with 6 items: couch, chair, desk, plant, rug, window (Fig. 1A). Stimuli were created using the *Space Designer 3D* website (https://www.spacedesigner3d.com). Four of the items (couch, chair, desk, plant, rug) changed location and configuration between the reinforced (CON+) and non-reinforced contexts (CON−), while the remaining two items (rug, window) remained in the same place across all stimuli. There was a single room configuration for CON+, but 6 different room configurations for CON− (Fig. 1B). These “feature-identical” contextual stimuli were designed to necessitate that distinguishing CON+ from the CON− could only be achieved through learning the overall CON+ configuration, and not by learning the location of a single element or pair of elements within CON+. The configural phase consisted of twelve 6-s presentations of CON+, and two 6-s presentations of each of the six CON− for a total of 12 CON− trials (see Fig. 1A). The US co-terminated with CON+ on 83% (10/12) of trials, but never with CON− or during ISI.

Elemental.—During the elemental conditioning phase two pictures of easily distinguishable cars (white car facing right, black care facing left) served as the conditional stimuli. The elemental phase consisted of eight 6-s presentations of the reinforced elemental conditional stimulus (CS+) and eight 6-s presentations of the non-reinforced elemental conditional stimulus (CS−) (see Fig. 1C). The US co-terminated with the CS+ on 83% (5/6) of trials, but never with CS− or during ISI. The color of CS+ and CS− (white, black) was counterbalanced across subjects.

2.3 Skin Conductance Response Measurement and Analysis

SCR was measured using a Biopac MP150 unit running Acqknowledge 4.3.1 software (Biopac Systems Inc., Goleta, CA) connected to an EDA100C-MRI amplifier with a 5 μS/V gain and a 10.0-Hz low-pass filter. Skin conductance signals were acquired using two Ag/AgCl 11mm electrodes (EL509) filled with isotonic recording electrode gel (GEL101) and placed on the thenar and hypothenar eminence of the left hand. Prior to electrode placement, the skin was lightly abraded. In each conditioning task skin conductance level (SCL) was recorded to the nearest microsiemens (μS) during each trial and ISI, with raw SCL data transformed through mean value smoothing. SCR magnitude was calculated as the difference between the mean SCL within the 2-second period prior to stimulus onset subtracted from the maximum SCL within 1–6 seconds following stimulus onset. SCR magnitudes were standardized within subject and across trials and conditions. Trials with outliers (± 3 standard deviations from the mean) were transformed through winsorizing (Wilcox & Keselman, 2003). SCRs were averaged into blocks of three trials for each

stimulus type. For CON+ and CON−, SCRs were averaged into “early” (trials 1–3), “early-middle” (4–6), “late-middle” (7–9), and “late” (10–12). For elemental CS+ and CS−, SCRs were averaged into “early” (trials 1–3) and “late” (trials 4–6).

2.4 MRI acquisition

MRI data were acquired using a 3T GE CXK4 scanner, which was equipped with 8 high-bandwidth receivers for ultra-short TR times in order to reduce signal distortions, and orbito-frontal signal dropout. High resolution T_1-weighted anatomical images were acquired using a spoiled gradient recalled echo sequence (FOV=25cm; matrix=256 × 256; 176 sagittal slices; 1mm thickness; TR=8ms; TE=4ms; flip angle=12°). Functional data were acquired using a T_2*-weighted echo planar image (EPI) sequence (matrix=64 × 64; 30 axial slices; in-plane resolution=3.43 × 3.43 × 2.6; gap=1.4mm; TR=1.5s; TE=32; flip-angle=90°).

2.5 fMRI preprocessing

Imaging analysis was conducted using FSL (Jenkinson et al., 2012) and AFNI (Cox, 1996). Identification of excessive motion artifact was conducted using independent component analysis (ICA) with FSL Melodic (Beckmann & Smith, 2004). Motion artifact-related activity was then removed (Kelly et al., 2010) and the motion-reduced images were entered into standard preprocessing using AFNI. The first 2 volumes of each EPI scan were removed and the remaining volumes were despiked, slice time and volume registered for residual motion-related artifact, and spatially normalized into MNI standard space. Datasets were visually inspected for quality assurance. EPI data were spatially smoothed (6-mm FWHM) and converted to percent signal change.

For the configural and elemental tasks, the CS+ and CS− trials were modeled separately using a six second boxcar function and convolved with the hemodynamic response. For both tasks, drift (linear and quadratic), motion (L/R, A/P, S/I, roll, pitch, yaw, and derivatives), censored time-points, and US onset were included as regressors of no interest. We also examined hippocampal and amygdala trial by trial activity. To do this, we modeled each trial as a separate regressor in a separate GLM. For configural trials, we extracted mean percent signal change from the ROIs (see below) for each trial and binned them into four trial blocks: Early, Mid-1, Mid-2, and Late (3 trials each bin) using SPSS (Version 22). For elemental threat acquisition, we binned the trials into two blocks: Early and Late (3 trials each bin).

2.6 Region of interest (ROI) definitions

Hippocampus and amygdala.—Primary hypothesis testing was focused on the a-priori region of the hippocampus (Acheson et al., 2012). The hippocampus ROI was anatomically defined from the left and right grey matter hippocampus masks from the Harvard-Oxford Probabilistic atlas. A secondary analysis was conducted to examine the extent to which the amygdala responds to configural and elemental threat learning. The amygdala ROI was also anatomically defined using the left and right amygdala mask from the Harvard-Oxford Probabilistic atlas. A paired-samples t-test, comparing CS+ versus CS− within the hippocampal and amygdala ROIs, was computed for both configural and elemental processing. These a-priori contrasts were thresholded ($p < .005$), and small volume corrected

(SVC; $p < .05$) within the volume of the hippocampus and amygdala using the AFNI *3dttest++ ClustSim* command with the updated –acf option as recommended by (Cox, Chen, Glen, Reynolds, & Taylor, 2017).

2.7 Whole-brain analyses

To further evaluate configural processing, we computed a whole-brain paired-samples t-test comparing CS+ and CS− trials, thresholded at $p < .005$; whole brain corrected ($p < .05$) using AFNI (Cox et al., 2017). We followed a similar procedure for the elemental conditions. To illustrate the unique and overlapping neural circuitry between configural and elemental processing, we created a map reporting: 1) unique configural clusters; 2) unique elemental clusters; 3) overlapping clusters.

2.8 Brain-SCR relationships

To assess the extent to which the identified ROI activity predicts configural and elemental learning, we correlated BOLD response from the identified hippocampus and amygdala clusters with the SCR. Specifically, we first computed maximum SCR differential scores, which were defined as the difference between the maximum SCR response for CON+ trials and the maximum response for CON− trials. Next, separate hippocampus and amygdala BOLD difference scores were similarly computed (configural CON+ minus configural CON−). SCR scores were then separately correlated with hippocampal and amygdala CON+ and CON− difference scores (Pearson 2-tailed). High scores reflect successful differential threat learning. An identical approach was used for elemental learning.

3. RESULTS

3.1 SCR

For configural threat acquisition there was a significant two-way Stimulus Type (CON+, CON−) × Block (early, early-middle, late-middle, late) interaction, $F(3,57) = 2.72$, $p = .05$. As shown in Fig. 2A, post-hoc comparisons revealed greater SCR for CON+ than CON− during the early-middle and late-middle blocks (ps < .019). SCR tended to decrease across blocks, $F(3,57) = 2.63$, $p = .06$. For elemental threat acquisition, there was a significant two-way Stimulus Type (CS+, CS−) × Block (early, late) interaction, $F(1,19) = 5.21$, $p = .034$. As seen in Fig. 2B, SCR for the CS+ was greater than the CS− in the late block, $p = .024$. During the elemental phase SCR also decreased across blocks, $p < .001$.

3.2 Hippocampus and amygdala results

As shown in Fig. 3A, a cluster in the left hippocampus significantly differentiated CON+ from CON− (SVC $p < .05$). The differentiation appeared strongest during early-middle trials ($p = .004$ Bonferroni corrected; Fig. 3B). This pattern was not observed for elemental threat learning (Fig. 3C). Specifically, there was no difference in hippocampal signaling between elemental CS+ and CS− during the first and second block of trials (Fig. 3D). In contrast to the hippocampus, the amygdala did not discriminate between configural CON+ and CON− (Fig. 4A). We observed that the amygdala habituated across both CON+ and CON− trial blocks without showing significant differentiation during any block (Fig. 4B). Conversely in the elemental task, amygdala activity was increased during CS+ trials compared to CS−

trials (SVC p<.05) (Fig. 4C). Amygdala activity was significantly greater in the CS+ trials than for the CS− during both the first and second block of trials (Fig. 4D).

3.3 Configural and elemental threat learning have shared and unique circuitry

Beyond the hippocampus and amygdala, configural threat acquisition is associated with a broader neural circuit including the prefrontal and parietal cortices (Glenn et al., 2017). To compare full circuit activation during these tasks, we conducted separate whole-brain voxel-wise paired samples t-test (voxel threshold, p<.005, and whole-brain cluster corrected, p<.05) comparing CON+ with CON− and elemental CS+ with CS− respectively (see Tables 1 and 2). To aid in identifying shared and unique neural circuitry associated with configural and elemental threat acquisition, we computed a 2-way cluster overlap map (Fig. 5). We found that the left and right superior parietal lobule (SPL), and a cluster in the left postcentral gyrus that extended into the left SPL was unique to configural threat acquisition. In contrast, we observed that the dorsal anterior cingulate cortex (dACC) was unique to elemental threat learning. Interestingly, the majority of the other clusters identified shared neural patterns between the two forms of learning. Specifically, a large cluster was observed in the left superior temporal gyrus (STG) for both configural and elemental threat learning. This large cluster extended into several regions including the rolandic operculum, postcentral gyrus, and mid/posterior portions of the insula, although for configural threat learning, the cluster extended into the inferior frontal gyrus but not for elemental threat learning. Both configural and elemental threat learning was found in the visual cortex, and brain-stem/periaqueductal grey area (PAG), Although, we observed that the brain-stem/PAG cluster extended into the posterior thalamus for configural learning, but not for elemental threat learning.

3.4 Brain-SCR results

The maximum CON+ versus CON− differential SCR scores did not correlate with differential configural CON+ versus CON− hippocampus or amygdala activity (rs < .27 ps > .24). This pattern was observed regardless of block (ps > .10). The same pattern was observed for the differential hippocampus and amygdala for elemental threat acquisition (rs < .01, ps >.96). As with findings for the configural phase, differential hippocampal and amygdala activity was not related to SCR across early or late elemental trials (ps > .48).

4. DISCUSSION

The aim of the current investigation was to delineate the neural mechanisms of configural threat acquisition and compare it to cued-based, or elemental, threat acquisition. We developed a novel “feature-identical” contextual threat acquisition task where configural CON+ and CON− were determined by the configuration of four elements in a room, in addition to a standard elemental cued conditioning task. Subjects demonstrated differential fear responding (SCR) to CS+/CS− trial types during both the configural and elemental tasks. Activity of the hippocampus, but not the amygdala, was significantly increased for the configural CON+ compared to the configural CON−. In contrast, the opposite pattern was observed for the elemental threat learning task — increased amygdala activity for elemental CS+ relative to elemental CS−, but no hippocampus differences. Moreover, using whole-

brain analyses, we found that configural and elemental threat learning have overlapping neural activity in several key fear expression neural regions, including the STG, posterior insula, sensory cortex, and the brain-stem/PAG.

Our results support the role of the hippocampus in configural threat acquisition. The hippocampus is thought to form a hierarchical configuration of a context by integrating the individual elements into a single cognitive and neural representation (Fanselow, 2000; Rudy, 2009). Pharmacological-lesion and optogenetic studies have demonstrated that disrupting the hippocampus impairs configural threat learning and memory retrieval (Anagnostaras, Gale, & Fanselow, 2001; Chang & Liang, 2017; Corcoran & Maren, 2001; Kheirbek et al., 2013; Phillips & LeDoux, 1992). The hippocampus is a key component of the contextual threat circuit (Maren et al., 2013; Rudy et al., 2004), sending contextual output-signals directly to the basolateral nucleus of the amygdala (BLA) and indirectly through the prelimbic cortex (dACC=human homologue) where a defensive response can be expressed via the central nucleus of the amygdala (CeA) and periaqueductal grey area (PAG) (Knapska et al., 2012; Maren et al., 2013). If the hippocampus is impaired, configural modulation of contextual processing is lost. This impairment leaves the BLA to take over contextual threat learning and results in elemental processing of contextual details (Iordanova, Burnett, Aggleton, Good, & Honey, 2009). A consequence of contextual learning via amygdala-driven, elemental processing is that a single cue then becomes capable of eliciting a generalized fear response in the future, even when encountered in isolation from the additional contextual information.

We did not find evidence that the amygdala significantly discriminated configural CON+ and configural CON− trials, but amygdala activity was associated with elemental threat learning. We expected to observe a role for the amygdala in configural threat acquisition due to its importance in threat learning (Büchel & Dolan, 2000; Davis & Whalen, 2001). Both the amygdala and the hippocampus have been observed in numerous contextual threat learning neuroimaging studies (Andreatta et al., 2015; Glenn et al., 2017; Lang et al., 2009). Furthermore, in a similar design as our study, Baeuchl et al. (2015) report differential amygdala response between configural CON+ and CON− trials. Although, the amygdala is not always a consistent finding as some neuroimaging investigations report a dissociation between the amygdala and the hippocampus for cued-based and contextual treat learning respectively (Marschner, Kalisch, Vervliet, Vansteenwegen, & Büchel, 2008). Nonetheless, our results suggesting that the amygdala plays a less prominent role in configural threat acquisition should therefore be taken cautiously. Future work will be necessary to delineate the amygdala’s role in configural threat learning.

The results of the whole-brain analyses indicate that there is considerable neural overlap between configural and elemental threat acquisition in the distributed fear circuit (Tovote, Fadok, & Luthi, 2015), including the STG, parietal cortex, visual cortex, sensory cortex, and brain-stem/PAG. The temporal cortex is implicated in the expression of fear, autonomic arousal, and contingency awareness (Critchley, Mathias, & Dolan, 2002), while the visual cortex increases in functional centrality during threat conditioning which may reflect enhanced processing of threat (Lithari, Moratti, & Weisz, 2016). The PAG is an important structure for outputting conditioned fear responses (Watson, Cerminara, Lumb, & Apps,

2016) in addition to sending US-related signals back to the amygdala, thereby forming an amygdalar-PAG circuit important for integrating prediction error responses during aversive conditioning (Herry & Johansen, 2014). In summary, our findings indicate that there is a similar neural architecture that underlies fear expression for configural and elemental threat acquisition.

Although our results demonstrate that the hippocampus plays an important role in configural threat acquisition, it is clear that more work remains. From a translational perspective, few studies have investigated the neural mechanisms associated with contextual threat acquisition in patients with PTSD (Greco & Liberzon, 2016; Steiger, Nees, Wicking, Lang, & Flor, 2015), and none to date have examined configural threat learning (Baeuchl et al., 2015; Glenn et al., in press). Therefore, future studies are needed in PTSD and other patient populations thought to have dysfunctional configural learning processes that may contribute to symptom development and maintenance (Acheson et al., 2012). From a methodological perspective, a potential fruitful approach would be to systematically modify the configural stimuli content by replacing individual configural CON+ elements with novel items, or presenting the CON+ configuration in a new background context. Investigation of this topic would be important for delineating the configural versus elemental processing boundaries associated contextual threat learning (Rudy, 2009), and the extent to which configural learning generalizes to similar configurations (Lissek, 2012). A noteworthy limitation is that we did not find a significant relationship between SCR and amygdala or hippocampal activity. Further investigation using additional behavioral (US expectancy, contingency awareness) and psychophysiological (e.g., fear potentiated startle, pupil dilation) measures of learning may help better delineate the link neural processes to online measures of configural threat acquisition (Acheson, Geyer, & Risbrough, 2014).

In conclusion, the present study provides novel evidence that the hippocampus is associated with configural threat acquisition, whereas the amygdala plays a stronger role in elemental threat learning. These results set the stage for a more detailed understanding of how contextual threat learning is instantiated in the brain — an important mechanism associated with PTSD and other fear-related disorders. and for the role of the hippocampus in the etiology, maintenance, and treatment of PTSD.

ACKNOWLEGEMENTS

This work was supported by the Center of Excellence for Stress and Mental Health and VA Merit Awards to VBR (IO1-BX002558) and ANS (I01-CX000292 & I01-CX000715) and VA Career Development Award to ADS (IK2CX000864). Writing of this manuscript was partially supported by the Office of Academic Affiliations, Advanced Fellowship Program in Mental Illness Research and Treatment, Department of Veterans Affairs.

REFERENCES

Acheson DT, Geyer MA, & Risbrough VB (2014). Psychophysiology in the Study of Psychological Trauma: Where are we Now and Where Do We Need to Be? In Kumari V, Bob P, & Boutros NN (Eds.), Current Topics in Behavioral Neurosciences (Vol. 21, pp. 157–183). Cham: Springer International Publishing. 10.1007/7854_2014_346 [PubMed: 25158622]

Acheson DT, Gresack JE, & Risbrough VB (2012). Hippocampal dysfunction effects on context memory: Possible etiology for posttraumatic stress disorder. Neuropharmacology, 62, 674–685. 10.1016/j.neuropharm.2011.04.029 [PubMed: 21596050]

Alvarez RP, Biggs A, Chen G, Pine DS, & Grillon C (2008). Contextual Fear Conditioning in Humans: Cortical-Hippocampal and Amygdala Contributions. Journal of Neuroscience, 28, 6211–6219. 10.1523/JNEUROSCI.1246-08.2008 [PubMed: 18550763]

Anagnostaras SG, Gale GD, & Fanselow MS (2001). Hippocampus and contextual fear conditioning: Recent controversies and advances. Hippocampus, 11, 8–17. https://doi.org/AID-HIPO1015>3.0.CO;2-7 [PubMed: 11261775]

Andreatta M, Glotzbach-Schoon E, Mühlberger A, Schulz SM, Wiemer J, & Pauli P (2015). Initial and sustained brain responses to contextual conditioned anxiety in humans. Cortex, 63, 352–363. 10.1016/j.cortex.2014.09.014 [PubMed: 25460498]

Andreatta M, Neueder D, Glotzbach-Schoon E, Mühlberger A, & Pauli P (2017). Effects of context preexposure and delay until anxiety retrieval on generalization of contextual anxiety. Learning & Memory, 24, 43–54. 10.1101/lm.044073.116 [PubMed: 27980075]

Baeuchl C, Meyer P, Hoppstädter M, Diener C, & Flor H (2015). Contextual fear conditioning in humans using feature-identical contexts. Neurobiology of Learning and Memory, 121, 1–11. 10.1016/j.nlm.2015.03.001 [PubMed: 25792231]

Barrett J, & Armony JL (2009). Influence of trait anxiety on brain activity during the acquisition and extinction of aversive conditioning. Psychological Medicine, 39, 255–265. 10.1017/S0033291708003516 [PubMed: 18466667]

Beckmann CF, & Smith SM (2004). Probabilistic independent component analysis for functional magnetic resonance imaging. IEEE Transactions on Medical Imaging, 23, 137–152. 10.1109/TMI.2003.822821 [PubMed: 14964560]

Büchel C, & Dolan RJ (2000). Classical fear conditioning in functional neuroimaging. Current Opinion in Neurobiology, 10, 219–223. 10.1016/S0959-4388(00)00078-7 [PubMed: 10753800]

Chang S-D, & Liang KC (2017). The hippocampus integrates context and shock into a configural memory in contextual fear conditioning. Hippocampus, 27, 145–155. 10.1002/hipo.22679 [PubMed: 27806432]

Chun MM, & Phelps EA (1999). Memory deficits for implicit contextual information in amnesic subjects with hippocampal damage. Nature Neuroscience, 2, 844–847. 10.1038/12222 [PubMed: 10461225]

Corcoran KA, & Maren S (2001). Hippocampal Inactivation Disrupts Contextual Retrieval of Fear Memory after Extinction. The Journal of Neuroscience, 21, 1720–1726. http://www.jneurosci.org/content/21/5/1720.abstract [PubMed: 11222661]

Cox RW (1996). AFNI: Software for Analysis and Visualization of Functional Magnetic Resonance Neuroimages. Computers and Biomedical Research, 29, 162–173. 10.1006/cbmr.1996.0014 [PubMed: 8812068]

Cox RW, Chen G, Glen DR, Reynolds RC, & Taylor PA (2017). FMRI Clustering in AFNI: False-Positive Rates Redux. Brain Connectivity, 7, 152–171. 10.1089/brain.2016.0475 [PubMed: 28398812]

Critchley HD, Mathias CJ, & Dolan RJ (n.d.). Fear Conditioning in Humans. Neuron, 33, 653–663. 10.1016/S0896-6273(02)00588-3

Davis M, & Whalen PJ (2001). The amygdala: vigilance and emotion. Molecular Psychiatry, 6, 13–34. [PubMed: 11244481]

Eichenbaum H, & Cohen NJ (n.d.). Can We Reconcile the Declarative Memory and Spatial Navigation Views on Hippocampal Function? Neuron, 83, 764–770. 10.1016/j.neuron.2014.07.032

Fanselow MS (2000). Contextual fear, gestalt memories, and the hippocampus. Behavioural Brain Research, 110, 73–81. 10.1016/S0166-4328(99)00186-2 [PubMed: 10802305]

Glenn DE, Risbrough VB, Simmons AN, Acheson DT, & Stout DM (2017). The Future of Contextual Fear Learning for PTSD Research: A Methodological Review of Neuroimaging Studies. Current Topics in Behavioral Neurosciences. 10.1007/7854_2017_30

Greco JA, & Liberzon I (2016). Neuroimaging of Fear-Associated Learning. Neuropsychopharmacology, 41, 320–334. 10.1038/npp.2015.255 [PubMed: 26294108]

Herry C, & Johansen JP (2014). Encoding of fear learning and memory in distributed neuronal circuits. Nature Neuroscience, 17, 1644–1654. 10.1038/nn.3869 [PubMed: 25413091]

Iordanova MD, Burnett DJ, Aggleton JP, Good M, & Honey RC (2009). The role of the hippocampus in mnemonic integration and retrieval: complementary evidence from lesion and inactivation studies. European Journal of Neuroscience, 30, 2177–2189. 10.1111/j.1460-9568.2009.07010.x [PubMed: 20128853]

Kelly RE, Alexopoulos GS, Wang Z, Gunning FM, Murphy CF, Morimoto SS, … Hoptman MJ (2010). Visual inspection of independent components: Defining a procedure for artifact removal from fMRI data. Journal of Neuroscience Methods, 189, 233–245. 10.1016/j.jneumeth.2010.03.028 [PubMed: 20381530]

Kheirbek MA, Drew LJ, Burghardt NS, Costantini DO, Tannenholz L, Ahmari SE, … Hen R (2013). Differential Control of Learning and Anxiety along the Dorsoventral Axis of the Dentate Gyrus. Neuron, 77, 955–968. 10.1016/j.neuron.2012.12.038 [PubMed: 23473324]

Knapska E, Macias M, Mikosz M, Nowak A, Owczarek D, Wawrzyniak M, … Kaczmarek L (2012). Functional anatomy of neural circuits regulating fear and extinction. Proceedings of the National Academy of Sciences, 109, 17093–17098. 10.1073/pnas.1202087109

Lang S, Kroll A, Lipinski SJ, Wessa M, Ridder S, Christmann C, … Flor H (2009). Context conditioning and extinction in humans: Differential contribution of the hippocampus, amygdala and prefrontal cortex. European Journal of Neuroscience, 29, 823–832. 10.1111/j.1460-9568.2009.06624.x [PubMed: 19200075]

LeDoux JE (2000). Emotion Circuits in the Brain. Annual Review of Neuroscience, 23, 155–184. 10.1146/annurev.neuro.23.1.155

Liberzon I, & Abelson JL (2016). Context Processing and the Neurobiology of Post-Traumatic Stress Disorder. Neuron, 92 14–30. 10.1016/j.neuron.2016.09.039 [PubMed: 27710783]

Lissek S (2012). Toward an account of clinical anxiety predicated on basic, neurally mapped mechanisms of Pavlovian fear-learning: The case for conditioned overgeneralization. Depression and Anxiety, 29, 257–263. 10.1002/da.21922 [PubMed: 22447565]

Lithari C, Moratti S, & Weisz N (2016). Limbic areas are functionally decoupled and visual cortex takes a more central role during fear conditioning in humans. Scientific Reports, 6, 29220. 10.1038/srep29220 [PubMed: 27381479]

Maren S, Aharonov G, & Fanselow MS (1997). Neurotoxic lesions of the dorsal hippocampus and Pavlovian fear conditioning in rats. Behavioural Brain Research, 88, 261–274. 10.1016/S0166-4328(97)00088-0 [PubMed: 9404635]

Maren S, Phan KL, & Liberzon I (2013). The contextual brain: implications for fear conditioning, extinction and psychopathology. Nature Reviews Neuroscience, 14, 417–428. 10.1038/nrn3492 [PubMed: 23635870]

Marschner A, Kalisch R, Vervliet B, Vansteenwegen D, & Büchel C (2008). Dissociable Roles for the Hippocampus and the Amygdala in Human Cued versus Context Fear Conditioning. The Journal of Neuroscience, 28, 9030–9036. http://www.jneurosci.org/content/28/36/9030.abstract [PubMed: 18768697]

Monti JM, Cooke GE, Watson PD, Voss MW, Kramer AF, & Cohen NJ (2015). Relating Hippocampus to Relational Memory Processing across Domains and Delays. Journal of Cognitive Neuroscience, 27, 234–245. 10.1162/jocn_a_00717 [PubMed: 25203273]

Nees F, & Pohlack ST (2014). Functional MRI studies of the hippocampus. Frontiers of Neurology and Neuroscience, 34, 85–94. [PubMed: 24777133]

Olsen R, Moses S, Riggs L, & Ryan J (2012). The hippocampus supports multiple cognitive processes through relational binding and comparison. Frontiers in Human Neuroscience, 6, 146. 10.3389/fnhum.2012.00146 [PubMed: 22661938]

Phillips RG, & LeDoux JE (1992). Differential contribution of amygdala and hippocampus to cued and contextual fear conditioning. Behavioral Neuroscience, 106, 274–285. 10.1037/0735-7044.106.2.274 [PubMed: 1590953]

Pohlack ST, Nees F, Ruttorf M, Schad LR, & Flor H (2012). Activation of the ventral striatum during aversive contextual conditioning in humans. Biological Psychology, 91, 74–80. 10.1016/j.biopsycho.2012.04.004 [PubMed: 22560888]

Rudy JW (2009). Context representations, context functions, and the parahippocampal–hippocampal system. Learning & Memory, 16, 573–585. 10.1101/lm.1494409 [PubMed: 19794181]

Rudy JW, Huff NC, & Matus-Amat P (2004). Understanding contextual fear conditioning: insights from a two-process model. Neuroscience & Biobehavioral Reviews, 28, 675–685. 10.1016/j.neubiorev.2004.09.004 [PubMed: 15555677]

Stark SM, Reagh ZM, Yassa MA, & Stark CEL (2017). What's in a context? Cautions, limitations, and potential paths forward. Neuroscience Letters. 10.1016/j.neulet.2017.05.022

Steiger F, Nees F, Wicking M, Lang S, & Flor H (2015). Behavioral and central correlates of contextual fear learning and contextual modulation of cued fear in posttraumatic stress disorder. International Journal of Psychophysiology, 98, 584–593. 10.1016/j.ijpsycho.2015.06.009 [PubMed: 26149734]

Tovote P, Fadok JP, & Luthi A (2015). Neuronal circuits for fear and anxiety. Nature Reviews. Neuroscience, 16, 317–331. 10.1038/nrn3945 [PubMed: 25991441]

Urcelay GP, & Miller RR (2014). The functions of contexts in associative learning. Behavioural Processes, 104, 2–12. 10.1016/j.beproc.2014.02.008 [doi] [PubMed: 24614400]

Watson TC, Cerminara NL, Lumb BM, & Apps R (2016). Neural correlates of fear in the periaqueductal gray. The Journal of Neuroscience, 36, 12707–12719. http://www.jneurosci.org/content/early/2016/11/09/JNEUROSCI.1100-16.2016.abstract [PubMed: 27974618]

Wilcox RR, & Keselman HJ (2003). Modern Robust Data Analysis Methods: Measures of Central Tendency. Psychological Methods, 8, 254–274. 10.1037/1082-989X.8.3.254 [PubMed: 14596490]

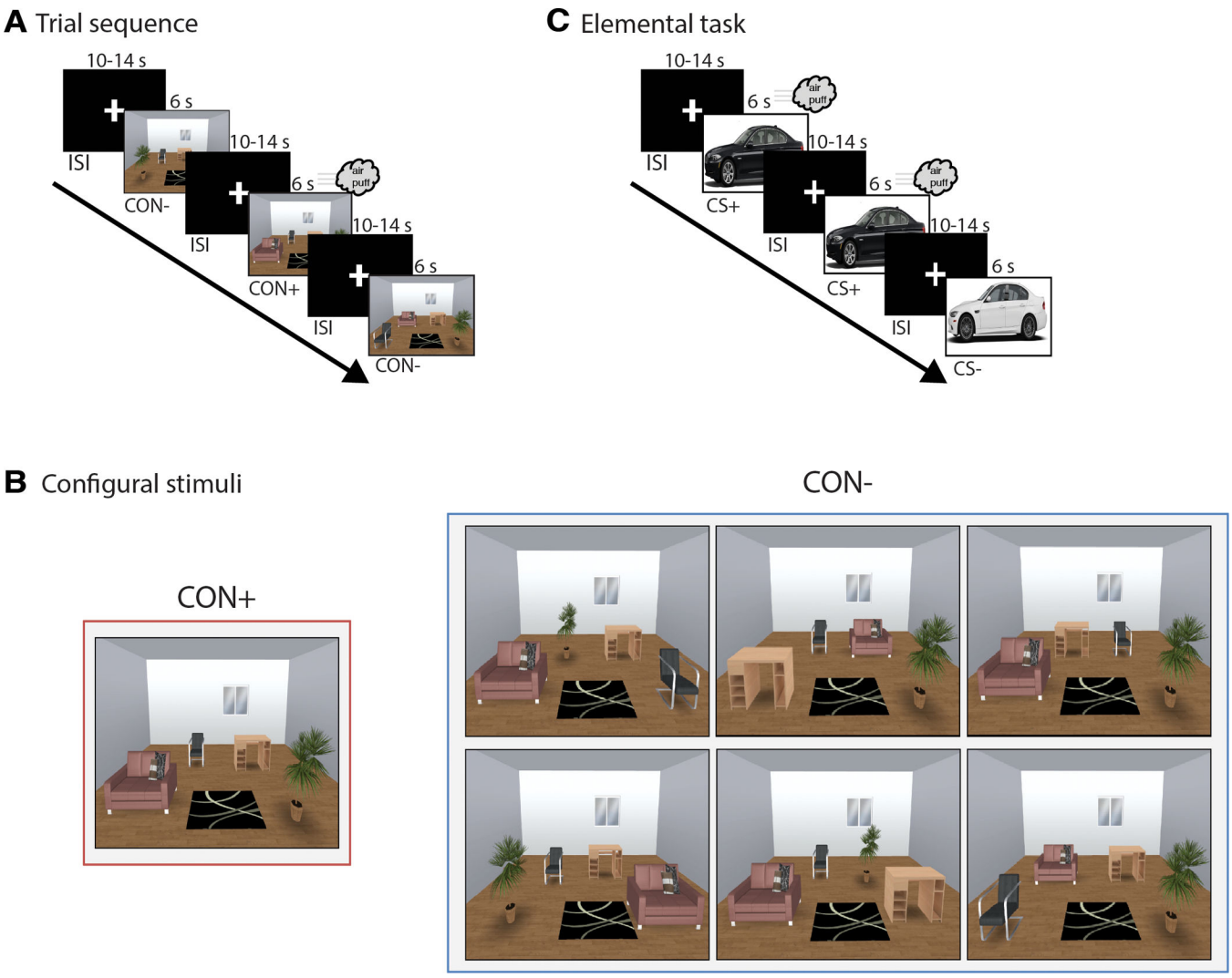

Fig. 1.

Configural and elemental threat learning tasks. (A) Trial sequence for the configural threat learning task. CON+ and CON− were presented for 6 seconds, followed by a 10–14 second ITI. The US co-terminated with CON+ on 83% of trials (see Methods for more details). (B) Examples for the CON+ and the different configurations of CON− trials. For CON− trials, each element was feature-identical to the CON+, but differed only on the arrangement of the furniture. CON− trial types were designed to minimize elemental processing. (C) Trial sequence for the elemental threat learning task. CS+ and CS− trials were presented for 6 seconds, followed by a 10–14 second ITI. The US co-terminated with the CS+ on 83% of trials.

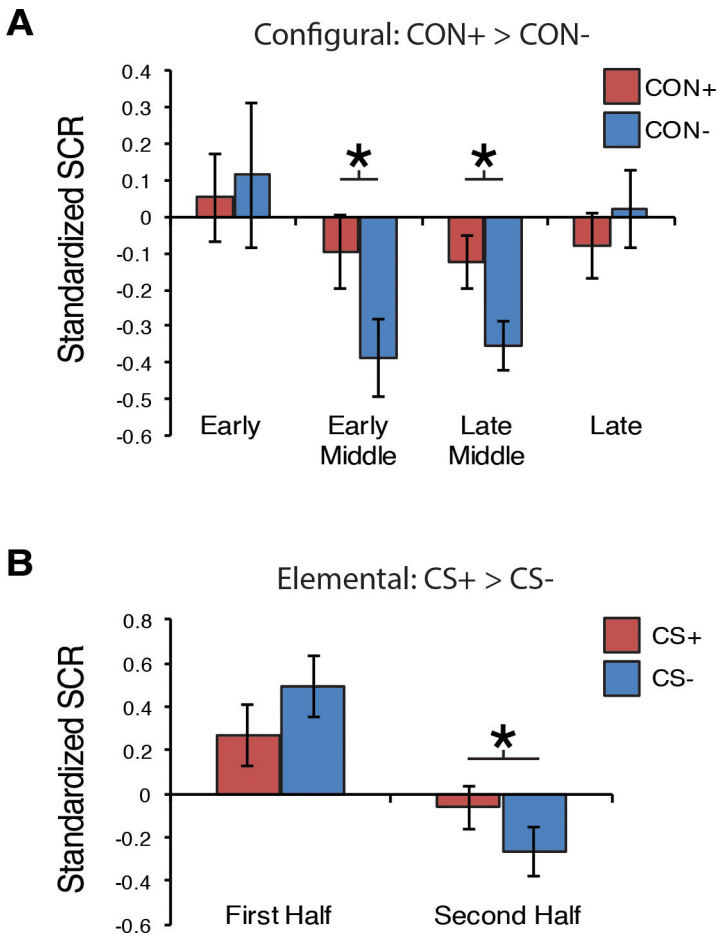

Fig. 2.

SCR results for configural and elemental threat learning. (A) Mean standardized SCR responses for configural treat learning across the four blocks (3 trials each block). (B) Mean standardized SCR for elemental threat acquisition across the first and second blocks (3 trials each block). Error bars=S.E.M. * < .05 (Bonferroni corrected).

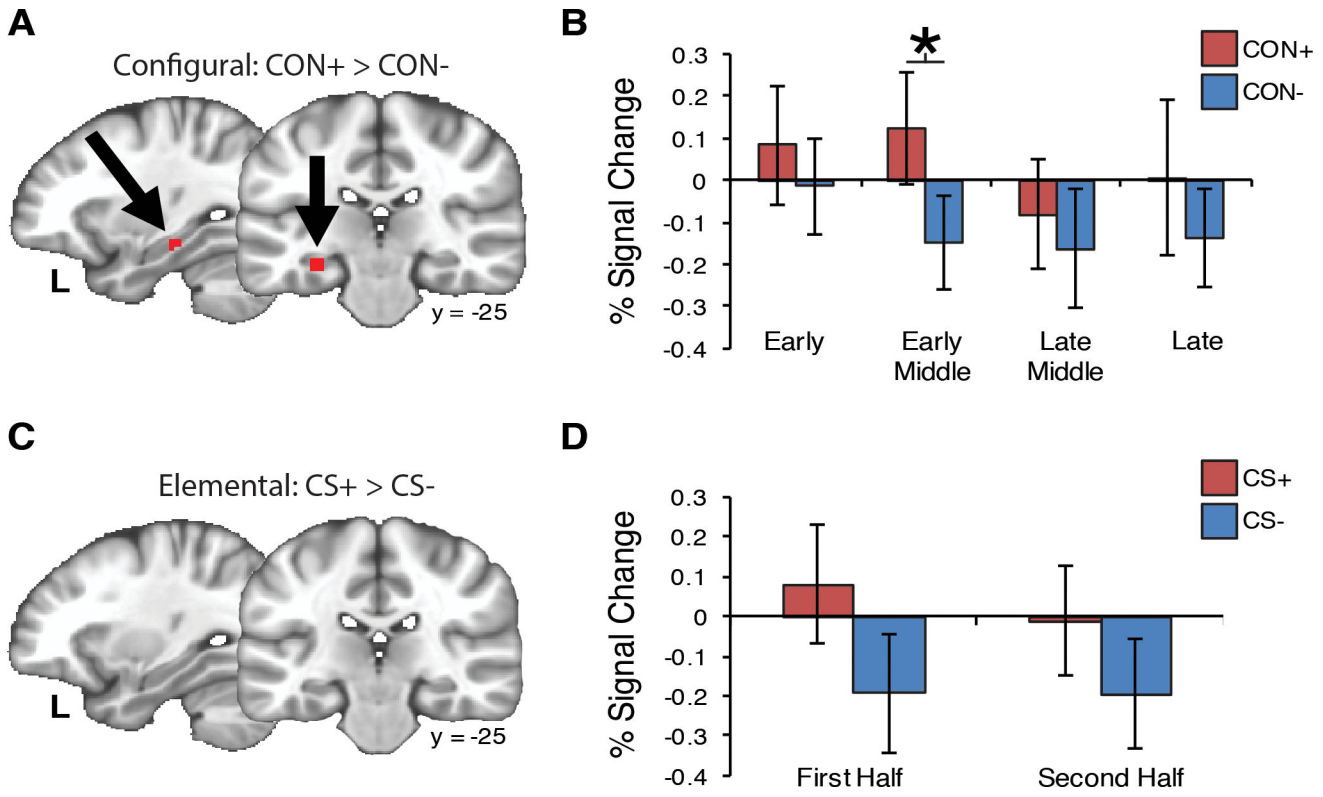

Fig. 3.

Hippocampus activity is associated with configural threat acquisition. (A) Hypothesis testing within the hippocampus ROI identified greater hippocampus activity for CON+ compared to CON− (MNI coordinates: x=−28, y=−25, z=−17; SVC $p < .05$; volume=5 voxels). (B) The difference between CON+ and CON− was strongest during the Early-Middle block of trials (p =004). (C) There was no difference for CS+ versus CS− during elemental threat learning, (D) regardless of the block of trials. Error bars=S.E.M. * < .05 (Bonferroni corrected).

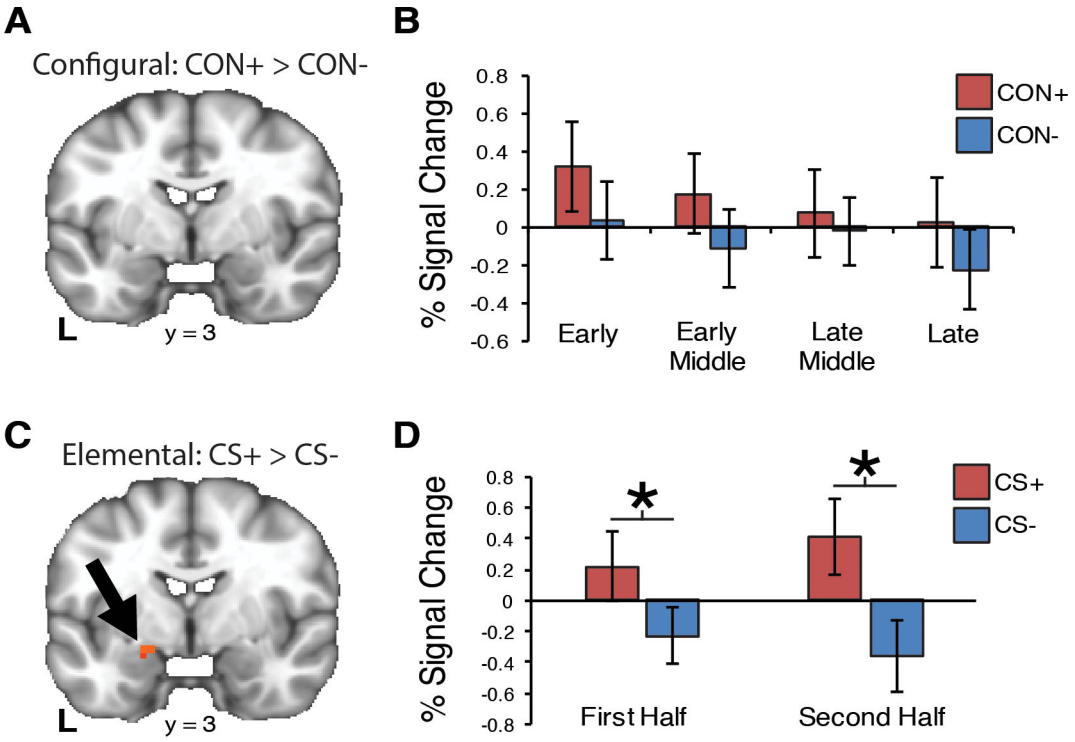

Fig. 4.

Amygdala ROI activity is associated with elemental but not configural threat acquisition. (A) For configural threat acquisition, the amygdala did not differentiate CON+ from CON−. (B) We observed a linear decrease in amygdala activity over the four blocks of trials. (C) An amygdala cluster was identified that differentiated CS+ and CS− trials (MNI coordinates: x=−17, y=3, z=−17; SVC $p < .05$; volume=6 voxels). (D) For elemental threat learning, amygdala was significantly increased for CS+ compared to CS− trials during both halves of learning. Error bars=S.E.M. * < .05 (Bonferroni corrected).

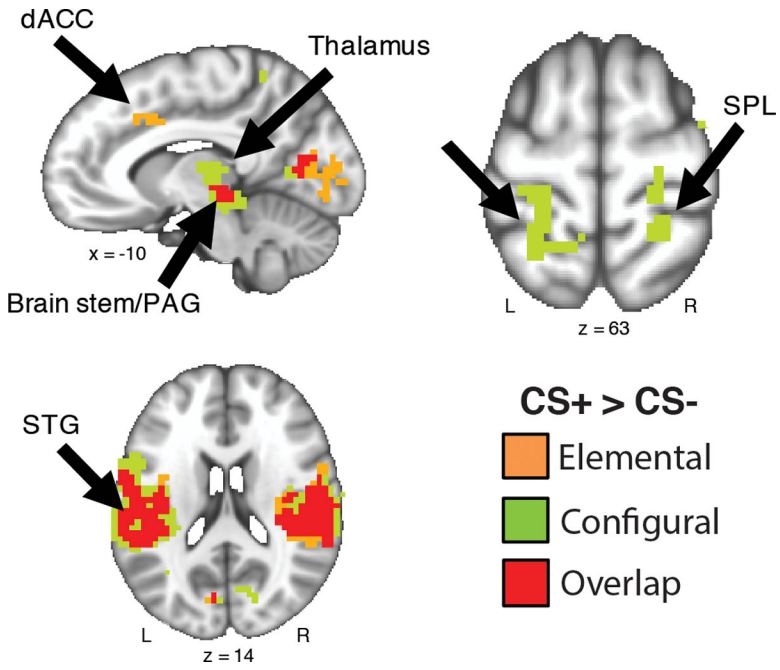

Fig. 5.

Configural and elemental threat learning have shared and unique neural activity. Results depict the whole-brain cluster overlap map of configural threat acquisition (CON+ versus CON− t-test; green clusters) and elemental threat acquisition (CS+ versus CS− t-test; orange clusters). The majority of regions observed overlapped between the two forms of threat learning (red clusters). Results are thresholded ($p < .001$) and corrected for multiple comparisons ($p < .05$). *Abbreviations*: dACC=dorsal anterior cingulate cortex; PAG=periaqueductal grey area; SPL=superior parietal lobule; STG=superior temporal gyrus.

Table 1.

Results of the whole-brain configural threat acquisition CON+ > CON− contrast

Region	x	y	z	Z Value	voxels
Left Superior Temporal Gyrus	−53	−29	11	6.81	1121
Inferior Frontal Gyrus	−56	13	14	3.41	-
Rolandic Operculum	−57	0	8	6.12	-
Mid Insula	−43	−1	9	4.94	-
Posterior Insula	−41	−14	3	4.85	-
Postcentral Gyrus	−59	−18	39	4.56	-
Right Supramarginal Gyrus	59	−18	18		823
Rolandic Operculum	52	1	8	5.11	-
Posterior Insula	39	−13	22	4.88	-
Superior Temporal Gyrus	51	−28	9	4.91	-
Postcentral Gyrus	56	−8	37	3.56	-
PAG/brain-stem	−7	−36	−10	4.58	282
Thalamus	−12	−22	9	4.13	-
Left Visual Cortex	−25	−64	7	4.77	166
Right Visual Cortex	21	−64	7	4.15	64
Left Post Central Gyrus	−20	−56	62	4.69	91
Left SPL	−26	−49	63	3.78	-
Right SPL	24	−46	63	4.00	86

Note: MNI coordinates of cluster peak responses. Z-Value reflects peak Z value within the cluster. Voxel-size=3.5mm^3. Cluster threshold $p < .005$; whole-brain cluster corrected $\alpha < .05$. PAG=periaqueductal gray; SPL=superior parietal lobule. CON+ = Contextual conditioned stimulus paired with the unconditioned stimulus (US; air-puff); CON− = Contextual conditioned stimulus not paired with the US.

Table 2.

Results of the whole-brain elemental threat acquisition CS+ > CS− contrast

Region	x	y	z	Z Value	voxels
Right Superior Temporal Gyrus	52	−29	14	4.84	595
Rolandic Operculum	53	−7	18	4.21	-
Posterior Insula	35	−27	21	3.71	-
Right Postcentral Gyrus	52	−11	37	3.70	-
Left Rolandic Operculum	−60	−4	11	5.30	481
Mid Insula	−37	−2	14	3.79	-
Superior Temporal Gyrus	−50	−32	12	4.19	-
Left Visual Cortex	−18	−88	−7	4.32	203
PAG/brain-stem	−11	−29	−7	3.99	91
Dorsal Anterior Cingulate Cortex	−4	13	39	4.04	87

Note: MNI coordinates of peak responses. Voxel-size=3.5mm^3. Z-Value reflects peak Z value within the cluster. Cluster thresholded $p < .005$; whole-brain cluster corrected $\alpha < .05$. PAG=periaqueductal gray. CS+ = elemental conditioned stimulus paired with US (air-puff); CS− = elemental conditioned stimulus not paired with US.